

P163

## Elasticity Tensor Inversion from Spherical Sample Measurements

D. Nadri (CSIRO Petroleum), A. Bóna\* (Curtin University of Technology) & M. Brajanovski (Curtin University of Technology)

### SUMMARY

---

From the P-wave traveltimes measurements over a spherical shale sample at 40 MPa we find the symmetry axis. We transform the ray velocities from the measurement coordinate system to the symmetry axis coordinate system. Assuming transverse isotropy symmetry, we estimate the elasticity tensor using a very fast simulated annealing algorithm followed by a quasi Newton method.

## Introduction

Due to sedimentation pattern of clay minerals, shale formations generally show transverse isotropy (TI) with vertical axis of symmetry. The main motivation of this study is to understand the seismic anisotropy of the overburden shale. Geological formations in the region under study are generally experiencing a horizontal stress field. This stress field may cause azimuthal anisotropy by either tilting the symmetry axis of shale formations and/or causing the directional planes of weakness. To characterize the seismic anisotropy, we have used P-wave traveltimes from a spherical shale core sample from the top of a sand reservoir. Unlike others, e.g Delinger (2005) and Vestrum and Brown (1994), we find the symmetry axis first and then invert for elasticity parameters to reduce the complexity of the inversion. Assuming TI symmetry, we have estimated the elasticity tensor using the simulating annealing followed by quasi Newton algorithm.

## Sample preparation and measurement

To prepare a spherical sample, a core sample was polished in different directions to obtain a sphere with 50 mm in diameter. The spherical sample has been placed in pressure chamber to measure the ultrasonic velocities in a broad range of confining pressures from ambient pressure to 700 MPa (Figure 1). Traveltimes are measured over the spherical sample at every 15 degrees in azimuthal and polar directions using the transducers at resonant frequency of 2 MHz (Figure 2). This acquisition pattern produced 132 records of P-wave traveltimes.



**Figure 1** Pressure chamber and spherical sample  
(Courtesy of Institute of Geology, Academy of Sciences, Prague)

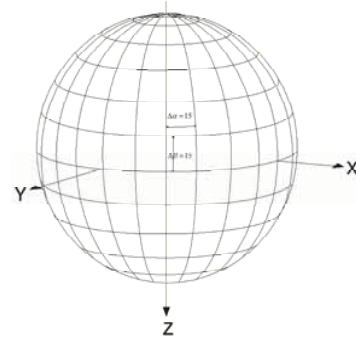


**Figure 2** A schematic of measurements locations on the sphere

## Estimation of major symmetry axis

To find the symmetry axis of a TI medium, we use the invariance of ray velocity  $V$  along the azimuthal direction, expressed by equation (1). To find the axis, we form an objective function  $S$  given by equation (2). This requires transforming the data from the measurement coordinates  $(\alpha, \beta)$  to the symmetry axis coordinates  $(\theta, \varphi)$  given by equations (3) and (4) with symmetry axis coordinates  $(\alpha_0, \beta_0)$ . This transformation is illustrated by Figure 3.

$$\left. \frac{\partial V}{\partial \varphi} \right|_{(\alpha_0, \beta_0)} = \frac{\partial \alpha}{\partial \varphi} \frac{\partial V}{\partial \alpha} + \frac{\partial \beta}{\partial \varphi} \frac{\partial V}{\partial \beta} = 0, \quad (1)$$

$$S(\alpha_0, \beta_0) = \sum_{\alpha=0}^{2\pi} \sum_{\beta=0}^{\pi} \left( \frac{\partial V}{\partial \varphi} \right)^2 / \left( \left( \frac{\partial \alpha}{\partial \varphi} \right)^2 + \left( \frac{\partial \beta}{\partial \varphi} \right)^2 \right), \quad (2)$$

$$\varphi = \tan^{-1} \left( \frac{-\sin \alpha_0 \cos \alpha + \cos \alpha_0 \sin \alpha}{\sin \beta_0 \cos \alpha_0 \cos \alpha + \sin \beta_0 \sin \alpha_0 \sin \alpha - \cos \beta_0 \tan \beta} \right), \quad (3)$$

$$\theta = \cos^{-1} (\cos \beta_0 \cos \alpha_0 \cos \beta \cos \alpha + \cos \beta_0 \sin \alpha_0 \cos \beta \sin \alpha + \sin \beta_0 \sin \beta), \quad (4)$$

$\frac{\partial \alpha}{\partial \varphi}$  and  $\frac{\partial \beta}{\partial \varphi}$  can be computed from equations (3) and (4).  $\partial V / \partial \alpha$  and  $\partial V / \partial \beta$  can be calculated numerically using the finite difference from measured ray velocities along the azimuthal and polar directions.

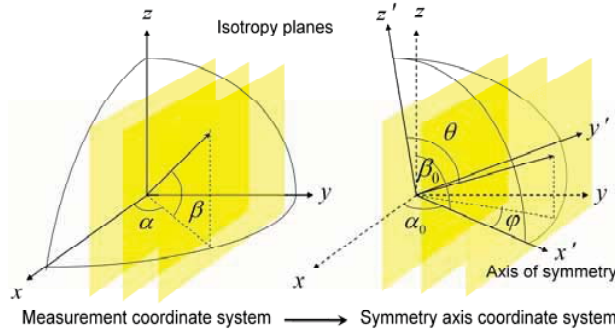


**Figure 3** Measurement and symmetry axis coordinate systems after rotation  $(\alpha_0, \beta_0)$ .

The objective function  $S$  is 2-dimensional and the direct searching of the model space could be used to find the solution instead of using other minimization algorithm. We draw prior values of  $\alpha_0$  and  $\beta_0$  from a uniform grid  $(0 \leq \alpha_0 \leq 2\pi, -\pi/2 \leq \beta_0 \leq \pi/2)$  and plotted the objective function in Figure 4. We used the ray velocities measured at 40 MPa pressure which is close to lithostatic pressure at the depth where the sample is taken from. Figure 4 shows the minimum of  $S$ , in northern hemisphere correspondent to the true solution. The second minimum is the projection of true one. Figure 5 shows the symmetry axis tilt, given by  $\beta_0 = 2^\circ$ ,  $\alpha_0 = 84^\circ$ .

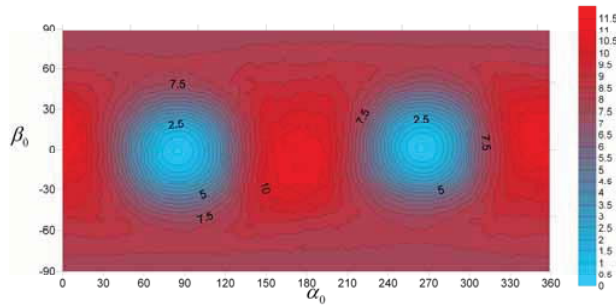


**Figure 4** Model space of the objective function  $S$ .

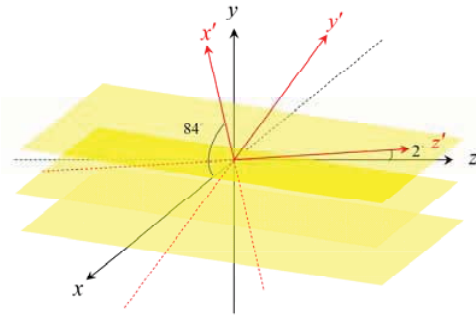


**Figure 5** The rotation of symmetry axis with respect to normal to bedding plane.

### Ray and Phase velocities and angles in TI medium

Phase velocity  $v$  for a quasi P-wave can be simply found by solving the Christoffel's equations for a TI medium. We use the same notation as given in Slawinski (2003),

$$v^2 = \left( (C_{33} - C_{11})n_3^2 + C_{11} + C_{44} + \sqrt{\Delta} \right) / 2\rho, \quad (5)$$

$$\Delta = \left( (C_{11} - C_{33})n_3^2 - C_{11} - C_{44} \right)^2 - 4 \left( C_{33}C_{44}n_3^2 - (2C_{13}C_{44} - C_{11}C_{33} + C_{13}^2)n_3^2(1 - n_3^2) + C_{11}C_{44}(1 - n_3^2)^2 \right),$$

$$n_3 = \cos \theta, \quad (6)$$

where  $C_{ij}$  are the elasticity coefficients,  $\rho$  is the density, and  $\theta$  is the phase angle. Hereafter we use normalized elasticity coefficients by density and wherever we refer to elasticity coefficients  $C_{ij}$ , they indeed are  $C_{ij} / \rho$ .

Because energy propagates with ray velocity, we use the following equation to relate ray and phase velocities,

$$V^2 = v^2 + (\partial v / \partial \theta)^2, \quad (7)$$

where  $V$  is the ray velocity and  $\partial v / \partial \theta$  can be expressed as a function of directional cosine  $n_3$ ,

$$\partial v / \partial \theta = -\sqrt{1 - n_3^2} \partial v / \partial n_3. \quad (8)$$

$\partial v / \partial n_3$  is simply the derivative of phase velocity (5) with respect to directional cosine  $n_3$ . To express  $n_3$  as a function of ray angle and ray velocity, we follow the same approach given in Ursin and Hokstad (2003),

$$n_3^2 = \left( \cos \alpha + \sin \alpha \frac{d \ln V}{d \alpha} \right) / \left( 1 + \left( \frac{d \ln V}{d \alpha} \right)^2 \right) \quad (9)$$

where  $\alpha$  is the ray angle.  $d \ln V / d \alpha$  can be simply found numerically using a four-term finite difference operator. Due to lack of enough measurements along the polar direction in each azimuth, we use linear interpolation for smaller  $\Delta \theta$ . Noise in measurements may cause instability in numerical differentiation. Hence, we fit a high order polynomial to the measured ray velocities and constrain it by  $\partial V / \partial \alpha|_{\alpha=0} = 0$ ,  $\partial V / \partial \alpha|_{\alpha=180} = 0$ . Figure 6 shows measured ray velocities in symmetry axis coordinate system in azimuth  $45^\circ$ . Figure 7 shows the numerically and analytically (polynomial fitting) calculated phase angles as a function of ray angle. The imposed constrained resulted in a more stable phase angles.

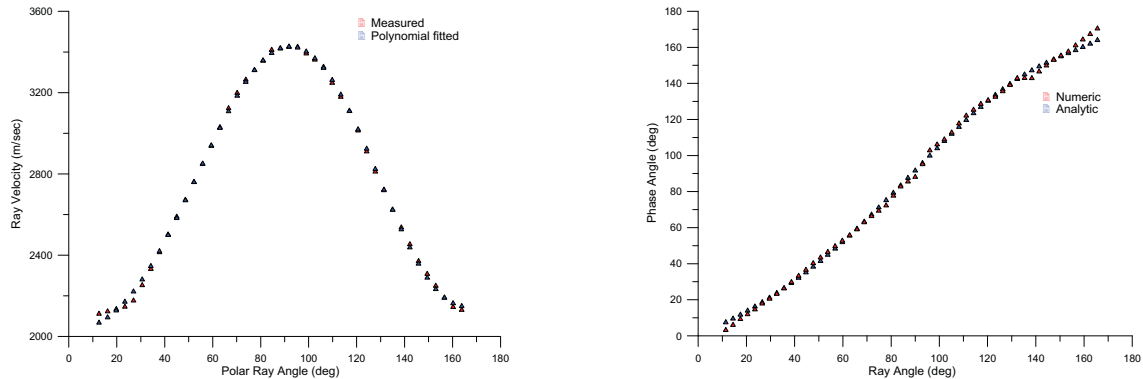


**Figure 6** Measured and polynomial fitted ray velocities. **Figure 7** Numeric and analytically computed phase angles.

### Inverse modelling and results

To minimize the objective function of the squared residuals of measured and computed ray velocities in symmetry axis coordinates, we implemented two different inversion algorithms. A very fast simulated annealing (VFSA) algorithm (Stofa and Sen, 1995) was used initially to get a solution close to global minimum from a prior model randomly drawn from a wide range uniform distribution for three elasticity coefficients  $C_{11}$ ,  $C_{13}$ , and  $C_{33}$ . Without the shear wave velocities it is impossible to uniquely estimate  $C_{13}$  and  $C_{44}$ . Hence, we kept  $C_{44}$  constant during the minimization. A prior value for  $C_{44}$  was estimated from the converted shear wave from a VSP survey. Following the VFSA we implemented a quasi Newton algorithm (Press et al., 2002) with a prior model set at the solution which was found from VFSA, to reach the exact solution quickly. Following are the normalized elasticity tensor elements and Thomsen anisotropy parameters for the sample at 40 MPa:

$C_{11} = 13.41$  GPa,  $C_{13} = 6.68$  GPa,  $C_{33} = 9.48$  GPa,  $\delta = 0.20$ , and  $\varepsilon = 0.21$ , where  $C_{44} = 2.25$  GPa.

Figure 8 shows the measured ray velocities in the symmetry axis coordinate system and Figure 9 shows the residual in the same coordinate system. As can be seen from these figures, TI symmetry assumption is valid. The residuals are in the range of measurement errors and there is no systematic error distribution.

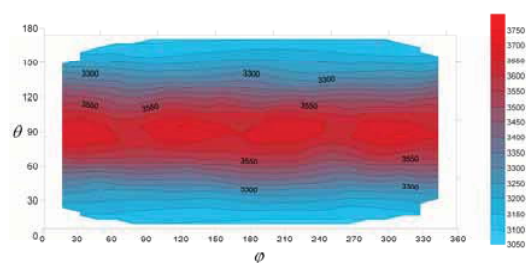


**Figure 8** Measured ray velocities in symmetry axis coordinate system.

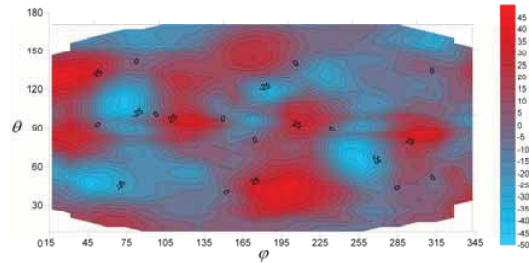


**Figure 9** Residual ray velocities in symmetry axis coordinate system.

## Conclusions

We have estimated the elasticity tensor for a spherical shale sample using the measured ultrasonic P-wave traveltimes in different azimuth and polar angles. We approximate the elasticity tensor using transverse isotropy symmetry and both ray velocities and especially ray velocity residuals confirm the validity of this assumption. To estimate the elasticity tensor, we used simulated annealing which followed by quasi Newton algorithm.

## Acknowledgment

We would like to thank BHP Billiton for partial financial support of this project in particular Guy Duncan for his support. We also acknowledge Tomáš Lokajčiek and his colleagues from Institute of Geology, Academy of Sciences in Prague, Czech Republic for making the spherical samples and ultrasonic measurements. We also thank, Boris Gurevich, Milovan Urosevic, and Maxim Lebedev from Curtin University of Technology for technical discussion, and lab measurements.

## References

- Dellinger, J., 2005. Computation of optimal transversely isotropic approximation of a general elastic tensor. *Geophysics*, 70, P. I1-I10.
- Press, W. H., S. A. Teukolsky, W. T. Vetterling, and B. P. Flannery, 2002. *Numerical recipes in C++ : the art of scientific computing*, Cambridge University Press.
- Slawinski, M. A., 2003. *Seismic waves and rays in elastic media*. Pergamon.
- Stoffa, P. L., and M. Sen, 1995. *Global optimization methods in geophysical inversion*. Elsevier.
- Ursin, B., and K. Hokstad, 2003. Geometrical spreading in a layered transversely isotropic medium with vertical symmetry axis. *Geophysics*, 68, 2082-2091.
- Vestrum, R., and R. J. Brown, 1994. From group or phase velocities to general anisotropic stiffness tensor. *CREWES Research Report*, 6, 10-1 – 10-16.